

Article

Efficient Multi-Material and High Deposition Coating including Additive Manufacturing by Tandem Plasma Transferred Arc Welding for Functionally Graded Structures

Gökhan Ertugrul ^{1,2,*} , Andre Hälsig ¹, Jonas Hensel ¹ , Johannes Buhl ² and Sebastian Härtel ²¹ Chair of Welding Engineering, Chemnitz University of Technology, 09126 Chemnitz, Germany² Chair of Hybrid Manufacturing, Brandenburg University of Technology Cottbus-Senftenberg, 03046 Cottbus, Germany

* Correspondence: goekhan.ertugrul@b-tu.de

Abstract: Market demands coating processes with high-performance, high reliability, high flexibility for processing of complex geometries and multi-material depositions, as well as increased deposition rates. The systematic coupling of two plasma transferred arc welding systems that interact in the same melt pool to form a tandem Plasma Transferred Arc (PTA) system accomplishes these tasks. Previous research has shown that the deposition rate with the tandem PTA method reaches 240 percent when comparing to the conventional single torch PTA method. Within one layer, up to four different powders and powder fractions can be combined at the same time. This allows for the creation of multi-material coatings that are suitable for sustaining high mechanical loads and wear- and temperature-resistant surfaces by use of tungsten carbides (WC). This study examines and analyzes defined functionally graded structures made from super duplex steel 1.4410 and corrosion resistant austenitic steel 1.4404. The mechanical-chemical properties of the tandem PTA system can be precisely controlled by changing the powder feeding positions. Furthermore, an additively manufactured specimen from previous studies is examined and evaluated. A direct comparison with conventional single torch PTA was performed to demonstrate the benefits of the tandem PTA-process.

Keywords: additive manufacturing; 3D Plasma Metal Deposition (3DPMD); austenitic stainless steel; super-duplex stainless steel; multi-material; functionally graded; high deposition rate; arc; powder



Citation: Ertugrul, G.; Hälsig, A.; Hensel, J.; Buhl, J.; Härtel, S. Efficient Multi-Material and High Deposition Coating including Additive Manufacturing by Tandem Plasma Transferred Arc Welding for Functionally Graded Structures. *Metals* **2022**, *12*, 1336. <https://doi.org/10.3390/met12081336>

Academic Editor: Aleksander Lisiecki

Received: 4 July 2022

Accepted: 3 August 2022

Published: 10 August 2022

Publisher's Note: MDPI stays neutral with regard to jurisdictional claims in published maps and institutional affiliations.



Copyright: © 2022 by the authors. Licensee MDPI, Basel, Switzerland. This article is an open access article distributed under the terms and conditions of the Creative Commons Attribution (CC BY) license (<https://creativecommons.org/licenses/by/4.0/>).

1. Introduction

Durability is a critical factor for a metallic component exposed to wear or corrosive environments. Surface modifications and choosing the proper manufacturing process are essential for mechanical components to increase their service time. In addition to lifetime, other limiting factors are cost, time pressure, geometric, and material constraints [1]. The challenge of providing high-efficient, high-performance, and safe coatings for complex geometries and components with flexible material depositions while increasing the deposition rate is driving the market increasingly. On the other hand, mechanical, thermal, and chemical effects such as crack formation, thermal stress, and intermetallic phase formation can be a hindrance in process selection. There are several suitable coating processes, including plasma transferred arc welding (PTA) [2], laser powder cladding, metal inert gas (MIG) welding, as well as tungsten inertia gas (TIG) cladding with wire material, thermal spraying, and others, each with its advantages and disadvantages [3]. In addition, PTA [4], wire arc additive manufacturing (WAAM) [5], laser powder cladding [6], and TIG [7] are suitable for the additive manufacturing process. Additive manufacturing may provide considerable advantages over traditional manufacturing and has transformative potential for various industrial applications [8]. The traditional production processes often require a considerable number of machining operations and are unable to satisfy the ever-increasing demands [9], which can be avoided by additive manufacturing. The motivation for additive

manufacturing is the need to reduce energy consumption, minimize waste material, and improve material efficiency [10]. PTA is a suitable method to require these motivation arguments in additive manufacturing.

In essence, PTA is a crucial surface modification process. The advantages of this method are its high deposition rate, controllable dilution rate, narrow heat-affected zone, and the utilization of a wide range of feed materials supplied in powder form. Furthermore, this process has the ability to fine-tune important cladding parameters such as powder feed rates, current, and heat input [11]. However, conventional PTA is not efficient enough for rapid production. Recent research shows that conventional PTA can be improved by development of the tandem PTA-process. Tandem PTA is fulfilled by the systematic coupling of two plasma transferred arc welding systems (Figure 1). Arc occurs between electrode and substrate, as well as powder feeding the melt pool (Figure 1a). Both coupled PTA systems are positioned in such a way that they act in a common melt pool (Figure 1c). Previous research has shown that the tandem PTA method can achieve a deposition rate of 240% when compared to the conventional single-torch PTA method [1]. Furthermore, bonding dissimilar metals, such as metal matrix composite deposition, is more efficient in tandem PTA in comparison with conventional PTA. In a study, the thermal decomposition of the WC hard material particles can be reduced, and the geometric distribution of the WC hard material particles can be positively influenced by varying the position of the hard material particle feed in the serial tandem PTA coating process. The percentage of WC hard particles of the cladded material is reached by a factor of 4 with tandem PTA in comparison to conventional PTA [12]. In another study, the application of additive manufacturing by tandem PTA has been tested and proven [13].

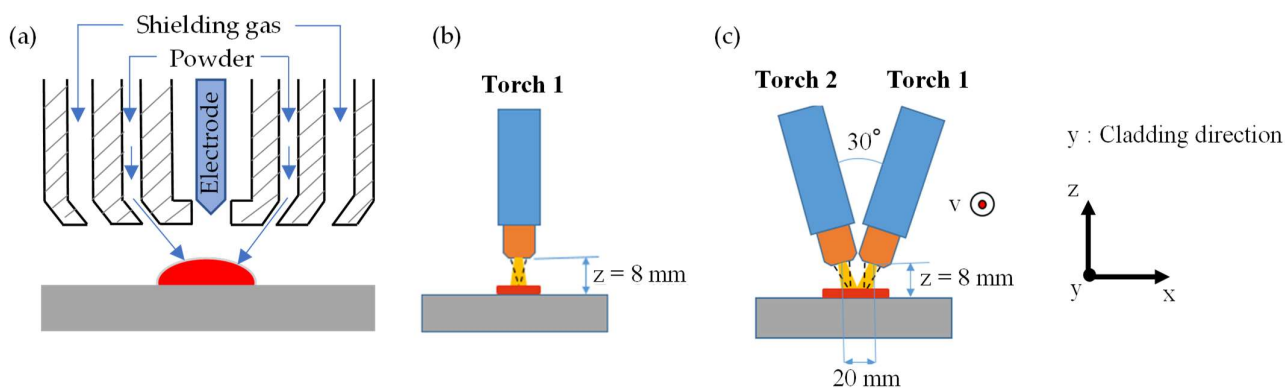


Figure 1. (a) Cross-section of torch conventional PTA (b) and tandem PTA (c) systems.

Both conventional PTA and tandem PTA systems offer the possibility of the combination of different metals in powder forms for coating and additive manufacturing. The combination of different powder metals in a common melt pool provides excellent bonding of dissimilar metals. Joining dissimilar metals is an effective way to achieve economic and better performance to produce graded structures with various methods. Both conventional PTA and tandem PTA methods provide excellent technology to optimize the properties of dissimilar materials and improve their functionality [14].

In particular, the joining of austenitic stainless steel and super-duplex stainless steel (SDSS) has received major attention in the industry as they offer better corrosion resistance and good mechanical properties. 1.4404 austenitic stainless steel is a low-carbon, high molybdenum content stainless steel grade that has a wide range of applications in oil and gas, petroleum, marine, and nuclear industries, and orthopedic implants in the bio-medical field. Similarly, super-duplex stainless steels exhibit higher yield and tensile strength, impact toughness, and demonstrate superior pitting and crevice corrosion resistance [15]. The component has to exhibit several properties to ensure corrosion and wear resistance. In this aspect, functionally graded materials (FGM) are excellent compositions to achieve desired features. Unlike conventional coated materials and composites, graded materials have a

continuous grade in composition between their respective end members. FGM utilizes the advantages of two different materials within one component [16]. The graded composition, such as continuous transition between different materials, improves the joint strength [4], reduces mechanical stress [17], thermal stress, and decreases the crack propagation potential [18] and cavitation-erosion, as well as erosion-corrosion resistance [19], which causes some mechanical and thermal problems. FGM eliminates many of the problems associated with discrete interfaces in conventional composites, such as poor mechanical integrity and transport losses due to low interfacial adhesion. It can also eliminate issues associated with thermal expansion mismatch, which is a significant problem for many conventional high temperature composites [20]. Despite its many advantages, the current research focuses on mono-material components, such as super duplex steel or austenitic corrosion resistance steels [4].

The aim of this study is to increase the deposition rate with two torches and to combine different materials in a single weld pool in order to build up a component with graded material. A direct comparison with conventional single torch PTA was performed to demonstrate the benefits of the tandem PTA-process. This study examines and analyzes defined functionally graded structures made from super duplex steel 1.4410 and corrosion resistant austenitic steel 1.4404. The mechanical-chemical properties of the tandem PTA system can be precisely controlled by changing the powder feeding positions. Furthermore, an additively manufactured specimen from previous studies is examined and evaluated [21]. A ship propeller is also used as an example to demonstrate the industrial application as an outlook.

2. Materials and Methods

2.1. Materials

An austenitic CrNi substrate with plate dimensions of $250 \times 100 \times 10 \text{ mm}^3$ was used. As filler materials in powder form (spherical, powder size $50\text{--}150 \mu\text{m}$), 1.4404 austenitic stainless steel and 1.4410 super duplex stainless steel were used. Table 1 shows the chemical composition of the substrate and powder.

Table 1. Chemical compositions of substrate and powder in wt% (1.4404) [4,22–24].

Material	Grade	C	Cr	Ni	Mn	Si	Mo	N	Fe
Substrate 1	1.4404	<0.03	18.5	13.0	<2.0	<1.0	2.0	<0.1	Balanced
Substrate 2	1.4301	<0.07	19.5	10.5	<2.0	<1.0	-	<0.1	Balanced
Powder 1	1.4404	0.03	16.6	12.6	0.4	0.8	2.1	<0.1	Balanced
Powder 2	1.4410	0.03	25.1	9.8	0.6	0.4	4.2	<0.1	Balanced

2.2. Methods

The tandem PTA system consists of two plasma welding power sources (Plasmastar GmbH, Griesheim, Germany), two PTA welding torches (MV230 with 3.2 mm Plasmastar electrodes), corresponding Plasmastar powder feed units, and a 6-axis Comau robot. The conventional PTA, on the contrary, consists of a single Plasmastar power source and a welding torch. Co-axially powder feeding torches are used in conventional PTA and tandem PTA.

An adjustable axis with three degrees of freedom for each torch was adapted to the robot arm as a torch holder, enabling both PTA welding torches to be positioned and fixed in place (see Figure 2).



Figure 2. Tandem PTA with handling system (TU Chemnitz).

Table 2 shows constant values of process parameters for the PTA and tandem PTA processes. Because of the high arc stability and the avoidance of atmospheric contamination, argon is used as a shielding gas with a 12 L/min flow rate for each torch. 1.4410 super duplex stainless steel with a relatively high hardness and 1.4404 austenitic stainless steel with a relatively low hardness are used as filler materials in powder form to obtain functionally graded materials. Each torch uses a 3 L/min powder gas flow rate to carry the powder to the melt pool. Substrate to torch distance is chosen at 8 mm for coating and 10 mm for additive manufacturing, as well as multi-material deposition, to avoid contamination of the torch by powder spatter. There is no significant difference between 1.4404 super duplex stainless steel and 1.4301 austenitic stainless steel. Therefore, 1.4404 is used for coating and multi-material deposition applications and 1.4301 is used for additive manufacturing.

Table 2. Constant values of the process parameters.

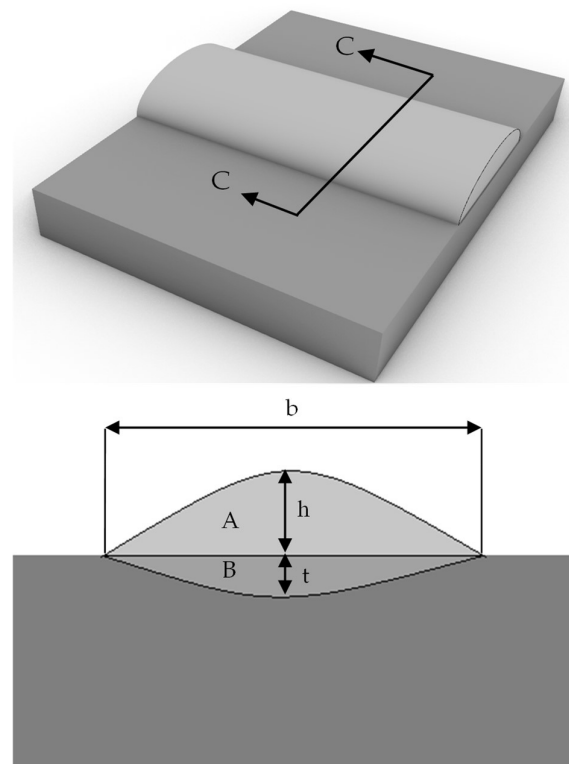
Constant Values	Parameters
Gas type	Argon
Shielding gas for each torch in L/min	12
Powder 1 type (50–150 μm)	1.4404
Powder 2 type (50–150 μm)	1.4410
Powder gas rate for each torch in L/min	3
Substrate-Torch distance in mm	8–10
Substrate 1 (Thickness 10 mm)	1.4404
Substrate 2 (Thickness 10 mm)	1.4301

2.2.1. Cross Section and Cladding Techniques

The dilution rate is used as an expression of the mixing of the two materials that occurs between the deposition and the workpiece [2]. The dilution rate is calculated according to Equation (1):

$$\text{Dilution} = 100 \times B / (A + B) [\%] \quad (1)$$

Figure 3 illustrates the C-C cross-section of the deposition application. B in mm^2 and h in mm are deposition area and reinforcement of deposition, A in mm^2 and t in mm are penetration area and penetration depth, and b in mm is the deposition width, respectively.

**Figure 3.** Schematic illustration of C-C cross-section of the weld seam.

In the stringer cladding method and wave cladding method, the weld bead is deposited in a straight line and with a zigzag formation, respectively (Figure 4). In this research, conventional PTA is used with the stringer cladding method, as well as tandem PTA, which is used for the stringer weld method.

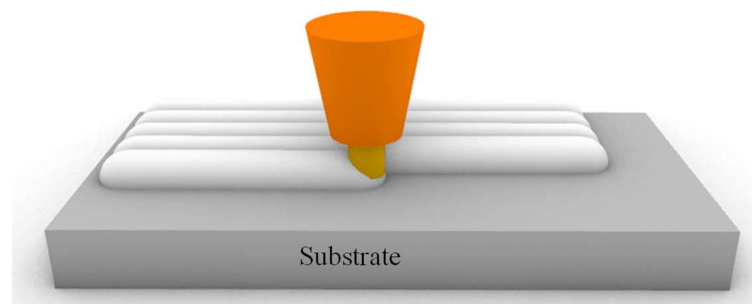


Figure 4. Stringer cladding method.

2.2.2. Parameters of the Torch Positions for Conventional PTA, Parallel Configuration Tandem PTA, and Series Configuration Tandem PTA

Figure 5 demonstrates the parameters and geometric positions of parallel configuration tandem PTA and series configuration tandem PTA for deposition. In the parallel configuration tandem method (a), two torches were moved parallel, and a symmetrical welding seam was created. A current of 140 A was applied for each torch and the angle between the two torches was set at 30° . The distance between the torches and the workpiece is 8 mm, and the distance between the central points of the torches is 20 mm. Two torches were moved consecutively in the series configuration in the tandem method (b), front and back torches. A current of 180 A and 90 A was applied for the front torch and the back torch, respectively. The front torch melts substrate and powder with a current of 180 A, and the back torch uses the heat of the front torch and supports the melting occurrence with a lower current of 90 A. The distance between the torches and the workpiece was 10 mm for a front torch and 13.5 mm for the back torch. The distance between the two torches was 20 mm, and an angle of 20° was set between them. Each torch has two powder feeding inlets. Both the front feeding inlet (shown in Figure 6 position 1, P1) and the back-feeding inlets (shown in position 2, P2) of torch 1 feed the material 1.4410. A similar setup is shown for torch two, where the front and back feeding inlets of torch two are stated as position 3 (P3) and position 4 (P4), respectively (Figure 6). The substrate material is 1.4404.

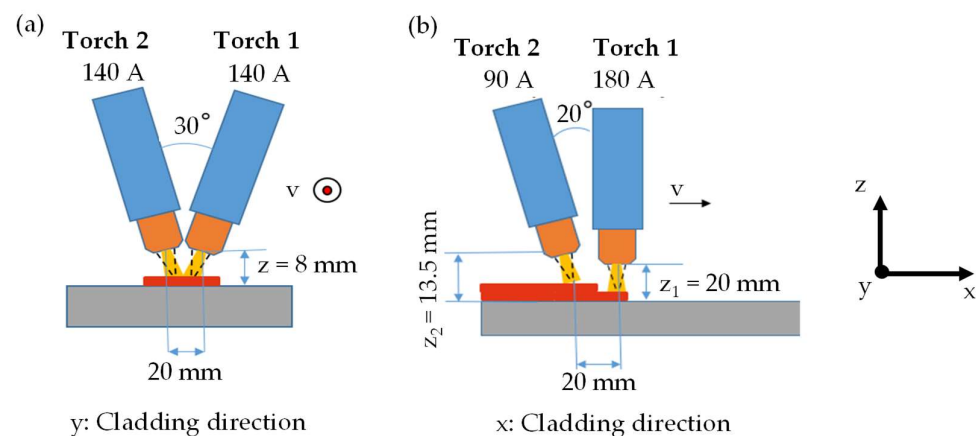


Figure 5. Parameters of the torches for (a) parallel configuration tandem PTA, (b) series configuration tandem PTA.

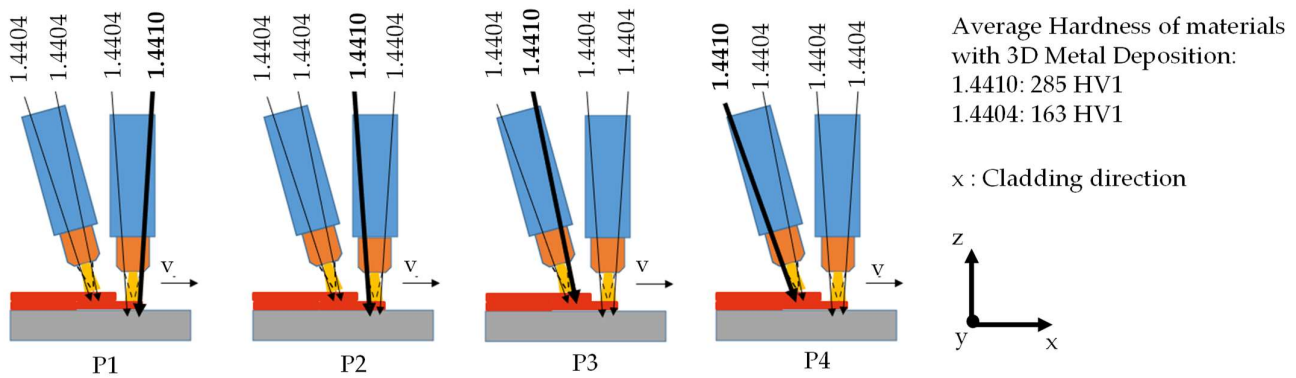


Figure 6. Powder feeding positions related with powder material 1.4410 (average hardness based on [4]) for each position.

2.2.3. Parameters of the Conventional PTA and Parallel Configuration Tandem Stringer PTA for High Deposition Coating

Table 3 illustrates cladding parameters of the conventional PTA stringer method, the conventional PTA wave method, and the parallel configuration tandem PTA stringer method. The conventional method consists of a single torch; therefore, it is used only as torch 1 during experiments with the position perpendicular to the substrate. For the conventional PTA stringer method, 150 A current, 14 cm/min cladding speed, and 23.5 g/min powder feeding rate are applied. By the conventional PTA wave method, 160 A current, 6 cm/min cladding speed, and 23.7 g/min powder feeding rate are applied. Unlike with other methods, 10 mm amplitude and 0.5 Hz frequency are used for the wave method. The tandem process employs two torches that work in tandem to build one weld seam. The total powder feed rate was 46.2 g/min, the cladding speed was 20 cm/min, and both torch currents were 140 A. A substrate of 1.4404 material was used.

Table 3. Cladding Parameters of the conventional PTA and Tandem PTA for coating.

Cladding Parameters	Conventional PTA Stringer	Parallel Configuration Tandem PTA Stringer
Current-Torch 1 in A	150	140
Current-Torch 2 in A	-	140
Cladding speed in cm/min	14	20
Total powder feeding rate in g/min	23.5	46.2
Plasma gas rate for each torch in L/min	2	2
Hatch distance in mm	7	12
Amplitude in mm	-	-
Frequency in Hz of wave method	-	-

2.2.4. Parameters of the Conventional PTA and Series Configuration Tandem PTA for Multi-Material Deposition

In comparison with conventional PTA stringers and series configuration tandem PTA for multi-material deposition, parameters were chosen to provide the same geometrical characteristic of the weld seam. As illustrated in Table 4, the same cladding speed of 40 cm/min, powder feeding rate of 51.50 g/min, and plasma gas rate of each torch of 2 l/min are applied for both methods. Torch 1 uses a current of 220 A for conventional PTA stringer method. Torch 1 and torch 2 are operated with 180 A and 90 A, respectively, for the tandem PTA stringer method in series configuration. 1.4404 material was used as substrate.

Table 4. Cladding parameters of conventional PTA and series configuration tandem PTA for multi-material coating.

Cladding Parameters	Conventional PTA Stringer	Series Configuration Tandem PTA Stringer
Current-Torch 1 in A	220	180
Current-Torch 2 in A	-	90
Cladding speed in cm/min	40	40
Total powder feeding rate in g/min	51.50	51.50
Plasma gas rate of each torch in L/min	2	2

Tandem P1, P2, P3, and P4 experiments were carried out to determine the effect of the powder feeding position with tandem PTA, as seen in Table 5. The total powder feeding rate for each experiment is 12.35 g/min for the material 1.4410 and 39.15 g/min for the material 1.4404.

Table 5. Powder position and current values of experiments for multi-material coating.

Method	Conventional PTA Stringer	Series Configuration Tandem PTA Stringer			
Experiment Name	Conventional P2	Tandem P1	Tandem P2	Tandem P3	Tandem P4
Positions of 1.4410 (Total 12.35 g/min)	P2	P1	P2	P3	P4
Positions of 1.4404 (Total 39.15 g/min)	Rest	Rest	Rest	Rest	Rest
Torch 1 Current in A	220	180	180	180	180
Torch 2 Current in A	-	90	90	90	90

2.2.5. Parameters of the Conventional PTA and Parallel Configuration Tandem PTA for High Deposition Additive Manufacturing

In the conventional PTA stringer method, 200 A current, 30 cm/min cladding speed, and 46.9 g/min powder feeding rate were utilized. The conditions used in the parallel configuration tandem PTA stringer method for high deposition additive manufacturing applications include 190 A current for each torch, 30° angle between torches, 40 cm/min cladding speed, and 97 g/min powder feeding rate, as seen in Table 6.

Table 6. Deposition parameters for high deposition additive manufacturing.

Deposition Parameters	Conventional PTA Stringer	Parallel Configuration Tandem PTA Stringer
Current-Torch 1 in A	200	190
Current-Torch 2 in A	-	190
Cladding speed in cm/min	30	40
Total powder feeding rate in g/min	46.9	97.0
Plasma gas rate of each torch in L/min	2	2

3. Results and Discussion

3.1. Part 1: Coating

3.1.1. Deposition Rate of Coating Tandem PTA and Conventional PTA

Figure 7 illustrates the cross-section of a single weld seam of conventional PTA (a) and tandem PTA (b). As a reference value, with $2.5 \text{ mm} \pm 0.5 \text{ mm}$ weld reinforcement and with 20 cm/min cladding speed, is taken to compare both methods for a single weld seam. For the conventional PTA stringer method, 150 A current, 20 cm/min cladding

speed, and 23.5 g/min powder feeding rate are applied. The weld width, reinforcement, and deposition area of conventional PTA are 8.01 mm, 2.4 mm, and 13.61 mm², respectively. With a weld width of 18.13 mm, tandem PTA is more than twice as wide as conventional PTA. For tandem PTA, each torch current is 140 A, the cladding speed is 20 cm/min, and the total powder feeding rate is 46.2 g/min. The weld reinforcement and deposition area are 2.43 mm and 29.94 mm² in tandem PTA.

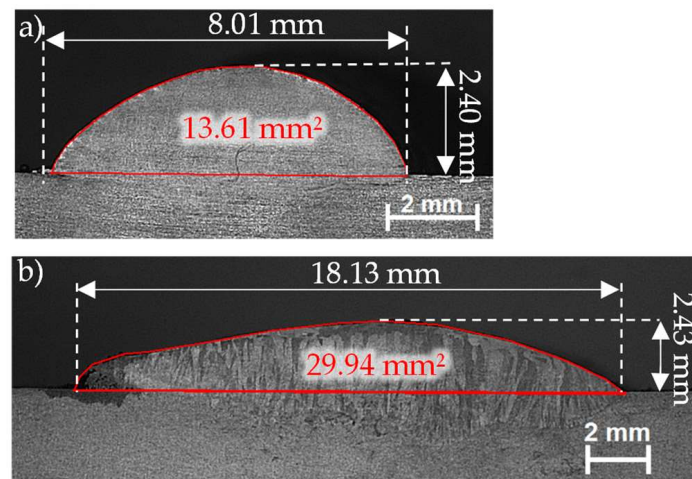
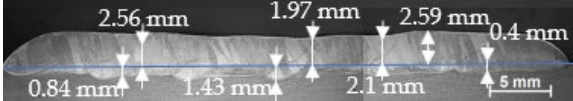
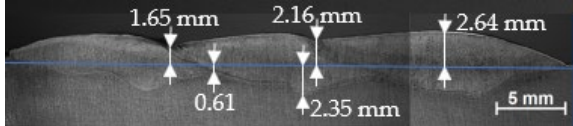


Figure 7. Cross-section of single weld seam of conventional PTA (a) and tandem PTA stringer (b).

Table 7 shows metallographic cross-section results and deposition efficiency factors for the conventional PTA stringer, PTA wave, and tandem PTA stringer. Each cross-section has a $95 \text{ mm}^2 \pm 10 \text{ mm}^2$ deposition area and a $2.1 \text{ mm} \pm 0.5 \text{ mm}$ deposition thickness. The deposition thickness and deposition area of the cross section were taken as a reference value to compare each method. The cladding parameters were chosen to achieve the same thickness. The deposition volume is used to calculate the coating capacity. The coating applied by the PTA stringer method was performed with six tracks and 7 mm offsets between each line in order to achieve a relatively flat surface. The cladding time for $A = 75 \text{ cm}^2$ was $t = 428 \text{ s}$. The time per cm² of coating was $t = 5.07 \text{ s}$. The maximum penetration depth, coating thickness, and dilution is 1.43 mm, 2.56 mm, and approximately 23%, respectively. The number of weld seams is lower than the conventional stringer PTA due to its large width. However, the local heat input is higher than that of conventional stringer PTA, resulting in increased workpiece distortion. The maximum penetration depth, coating thickness, and dilution are 1.36 mm, 2.45 mm, and approximately 27%, respectively. In the tandem PTA string method, the coating was performed with three tracks with a displacement of 12 mm between the lines. The maximum coating thickness and the dilution are 2.64 mm and ca. 30%, respectively. Two plasma torches focus on the same point; therefore, heat increases between the torches. At that point, the penetration depth increases with the highest value of 2.35 mm as a side effect. However, the heat between focused torches increases the powder melting amount simultaneously. In addition to this, the dilution is not constant in the cross sections due to heat accumulation for both processes. The coating time was $t = 179 \text{ s}$, which was the shortest coating time compared to the other method. The time per cm² of coating was $t = 2.39 \text{ s}$. Compared to the conventional PTA stringer method, the same area can be coated in 40% of the time with the tandem PTA. In other words, tandem PTA is capable of coating an area 2.4 times larger in the same amount of time as conventional stringer PTA.

Table 7. Multi-material coating is applied by the series configuration torches.

Method	Microscope Image of Cross Sections	Time per Coating (75 cm ² Area) in s/ Required Time in %	Coating Time per cm ² in s	Coating Capacity for the Specified Time in %
PTA stringer		(428 s)/ 100%	5.70	100%
Parallel configuration tandem PTA stringer		(179 s)/ 40%	2.39	240%

3.1.2. Effect of the Powder Feeding Position for Multi-Material Deposition

Multi-material coating is applied by the series configuration torches in tandem PTA and the stringer cladding method in conventional PTA. With the tandem PTA, four different powder feeding positions are available. Position 1 (P1) and position 2 (P2) are located on the first torch, as well as positions 3 (P3) and 4 (P4), which are located on the second torch regarding the 1.4410 material, shown in Figure 6. In addition, the comparison was made with conventional PTA with conventional P2. The dilution rate of samples is ca. 8% (Equation (1)).

By changing the powder feeding positions of the tandem PTA system, the ferritic content and the mechanical-chemical properties are adjusted specifically. The hardness test of clad material and substrate was applied between 13 and 15 points with HV1, including a near surface hardness map constituted of 114 points. The average hardness of the additively manufactured materials 1.4404 and 1.4410 by 3D Plasma metal deposition described in the literature is 163 HV1 and 280 HV1, respectively. The reason is that increased ferrite content in the microstructure leads to increased strength [4]. From this point of view, it is possible to use the Schaeffler diagram or the WRC-92 diagram and include the hardness relationship Figure 8. This diagram highlights that material composition changes with Cr equilibrium, Ni equilibrium, and ferrite content. Furthermore, 1.4404 contains an austenitic phase without ferrite content, whereas 1.4410 contains around 35% ferrite. The short diagonal dashed line between 1.4404 and 1.4410 shows the expectative composition of multi-material deposition.

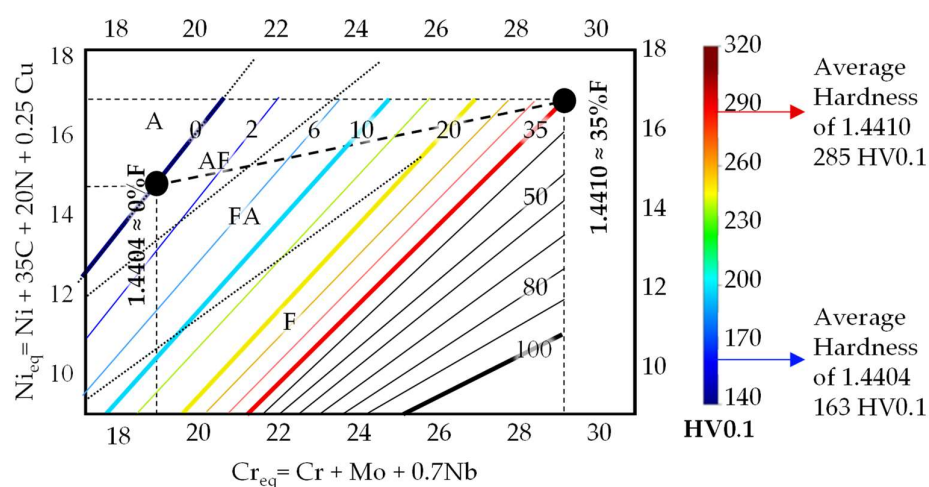


Figure 8. WRC-92 diagram of the raw materials revealing the transition from duplex to austenitic structure (A = austenite, AF = austenite + ferrite, FA = ferrite + austenite, F = ferrite) based on [4,25] with hardness scale used for the following hardness measurements.

Figure 9 shows the hardness and cross-section of the sample of conventional PTA position 2. The hardness map and linear hardness indicate homogenous hardness with a maximum of 225 HV01 and relatively high clad material hardness with an average of 205 HV1 in comparison with the following other samples. The reason for homogenous coating is that 1.4410 material dissolves due to the feeding back inlet of a single torch (P2) in the melt pool. Thus, the mixture of the austenitic stainless steel 1.4404 and the super duplex stainless steel 1.4410 is relatively high in the clad material. Linear hardness indicates a sharp transition of hardness between the weld and the substrate.

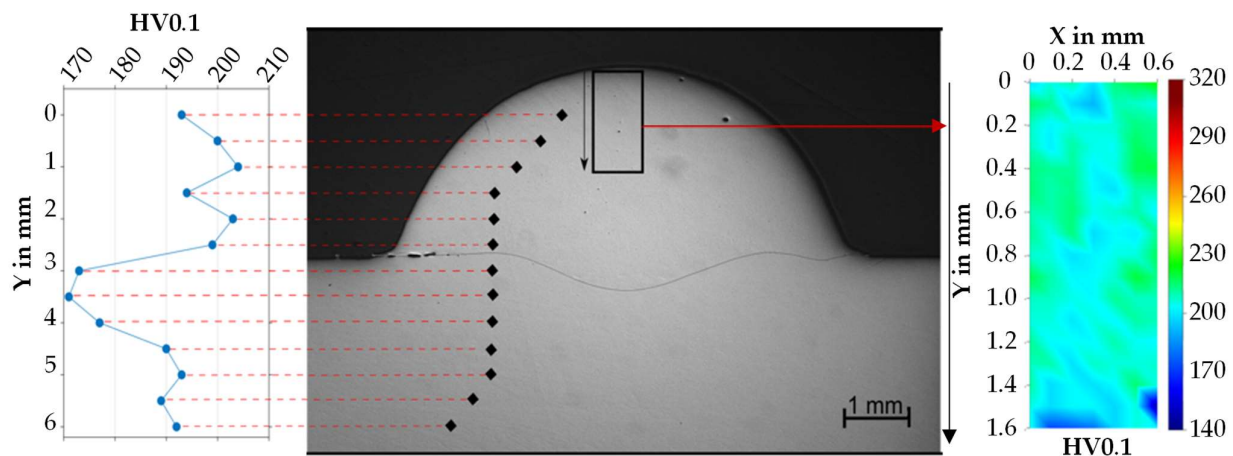


Figure 9. Cross-section and result of the hardness measurement of the sample conventional P2 (P2, I1 = 220 A).

Figure 10 shows the hardness and cross-section of the sample tandem PTA, which has powder feeding position 1. 1.4410 material was applied by the feeding front inlet of torch 1 in the melt pool. The remaining feeding inlets of both torches deposit the material 1.4404 on the material 1.4410 afterwards. Therefore, the lower part of the cross section of the coating indicates high hardness with approximately 205 HV0.1, as compared to the average clad material hardness and the surface hardness. The hardness map indicates a low surface hardness with a maximum of 214 HV01 and linear hardness indicates high clad material hardness, with an average of 190 HV1 as compared with other samples. Despite the deposition with two torches, the interface area between 1.4410 and 1.4404 materials does not exist. Linear hardness indicates a sharp transition of hardness between the weld and the substrate.

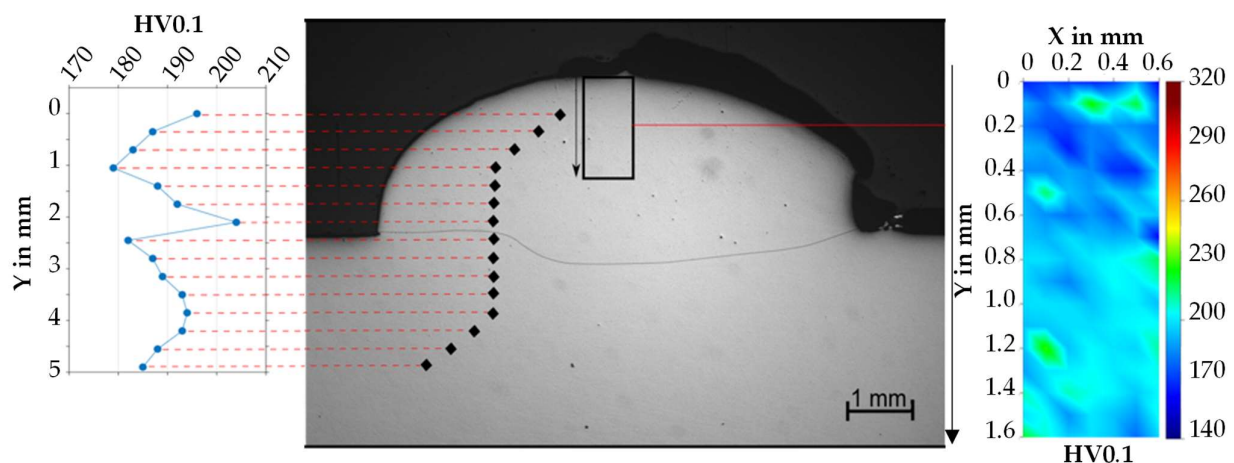


Figure 10. Cross-section and result of the hardness measurement of the sample tandem P1 (P1, I1 = 180 A, I2 = 90 A).

Figure 11 demonstrates the hardness and the cross-section of the sample tandem P4, which has a powder feeding position P4. Afterward, 1.4410 material is applied by the front and back inlets of torch 1 as well as the front inlet of torch 2 in the melt pool. Thereafter, the back inlet of torch 2 deposits 1.4410 material on the melt pool. Therefore, the hardness map indicates that the coating has high surface hardness with a maximum of 308 HV01 to achieve a high wear resistance attributed to the ferrite content. Linear hardness indicates the existing of a lower cladded material hardness with an average of 178 HV1 against the crack formation of coating through austenite content. A heterogeneous coating is the mixture of austenitic stainless steel and super duplex stainless steel that are low in the cladded material. The interface between the two materials, 1.4410 and 1.4404, cannot be distinguished, as indicated in the images. Linear hardness indicates a smooth transition of hardness between the weld and the substrate.

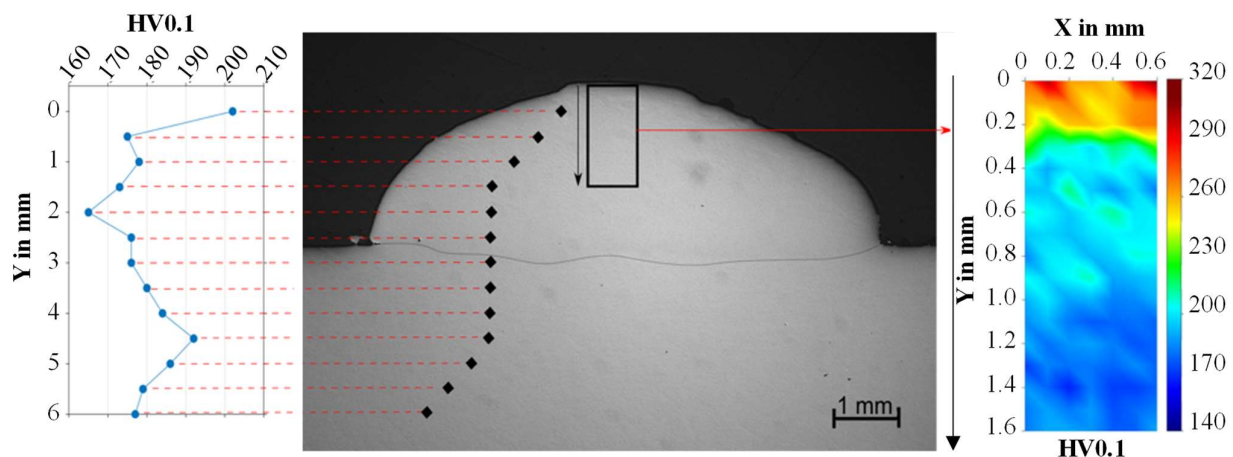


Figure 11. Cross-section and result of the hardness measurement of the sample tandem P4 (P4, I1 = 180 A, I2 = 90 A).

The result shows that the coating properties are adjustable by the changing powder feeding position for multi-material applications. Tandem PTA has more advantages for manipulating the mechanical-chemical properties than conventional PTA. It is possible to create a heterogenic structure in a single layer coating without an interface area. Relatively high surface hardness, including low cladded material hardness, was achieved by tandem PTA with P4 as well as P3.

3.2. Part 2: Additive Manufacturing

High Deposition Rate Additive Manufacturing by Conventional PTA and Tandem PTA

High deposition rate additive manufacturing is applied by the parallel configuration torches in tandem PTA and the stringer cladding method in conventional PTA, respectively. The general view of the additive manufactured wall by conventional PTA and parallel configuration tandem PTA methods is demonstrated in Figure 12. By tandem parallel configuration PTA, the torches create and feed the melt pool from both sides, symmetrically and simultaneously. The surface of the part performed with conventional PTA exhibits waviness and lack of symmetry (Figure 12a), resulting in lower geometric accuracy of the part. However, this is improved by the tandem PTA process, as illustrated in Figure 12b, where the deposition is equal for each layer. Therefore, the whole part conformance and geometry is more symmetrical and inline.

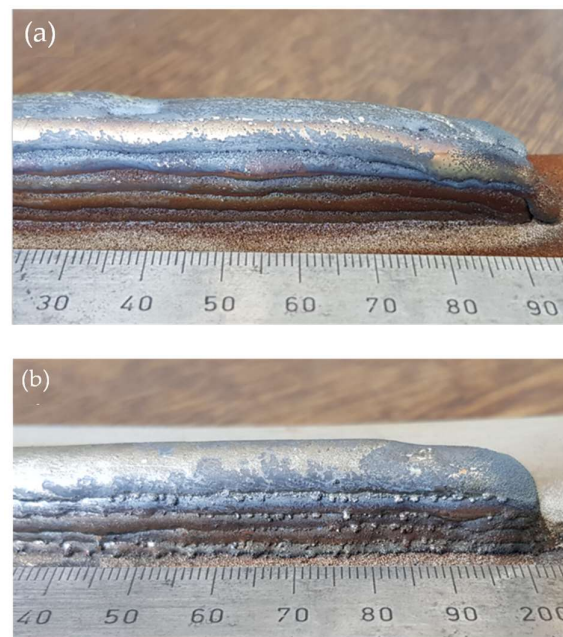


Figure 12. General view of additive manufactured wall by conventional PTA stringer (a) and parallel configuration tandem PTA (b) methods [21].

Figure 13 illustrates the cross section of the additive wall of the conventional PTA stringer method and the tandem PTA stringer method. The effective useful area of the samples is formed by determining the maximum effective width and height, respectively, which are shown by dashed lines. The reference deposition volume was 20 cm^3 with $h = 15 \pm 2 \text{ mm}$ height and $w = 9 \pm 0.5 \text{ mm}$ width of the effective area, which is demonstrated by optical microscope (OM, ZEISS, Chemnitz, Germany) images of cross sections of the classical PTA and the parallel configuration tandem PTA in Figure 13. The parameters were chosen to generate specific geometries and to reach the maximum cladding speed and the maximum deposition rate. The parameters specified are listed in Table 6. The interpass temperature was limited to a maximum of $200 \text{ }^\circ\text{C}$. In the conventional PTA, the torch was arranged 10 times to manufacture the wall. Each layer is composed of two welding passes that are configured separately. The width of the first layer is lower than the upper layers due to the high cooling rate, despite the interpass temperature. The bulges indicated in the cross section of the conventional PTA additively manufactured wall (Figure 13a,c) are more pronounced in comparison with the tandem PTA additively manufactured wall (Figure 13b,d). However, in the parallel configuration tandem PTA, 7 layers were welded with the parallel configuration twin torch. As an assumption, the accumulation of material deposited on one side is a cause of arc blowing due to the magnetic field of the two torches. The width of the first two layers is high due to the flat and high surface area of the substrate. The reason could be that upper additive layers have a lower deposition surface area during application due to the two torches being at an angle to each other. Furthermore, the focusing of the torches is constant and the layer height changes with each layer. This can lead to reduced efficiency and needs to be worked on it. Hence, the coating application with tandem PTA has an efficiency of 240% in comparison with conventional PTA, whereas additive manufacturing has an efficiency of 56%. The dilution with base material around 5% for both processes. However, the dilution of the top layer of the conventional PTA and tandem PTA increase to around 10% and 17%, respectively. In addition to this, the surface roughness of the tandem PTA additive wall is smoother in comparison with conventional PTA additive wall. The deposition time of the conventional PTA for 20 cm^3 was 280 s. The time per cm^3 was 14 s. The deposition time of the parallel configuration tandem PTA for 20 cm^3 was 182 s. The specified time does not consider interpass cooling time. The time per 1 cm^3 was 9 s. For comparison, the deposition capacity of the tandem PTA is 56%

higher than that of the conventional PTA for the specified time, and the total interface area between welds is less than the conventional PTA.

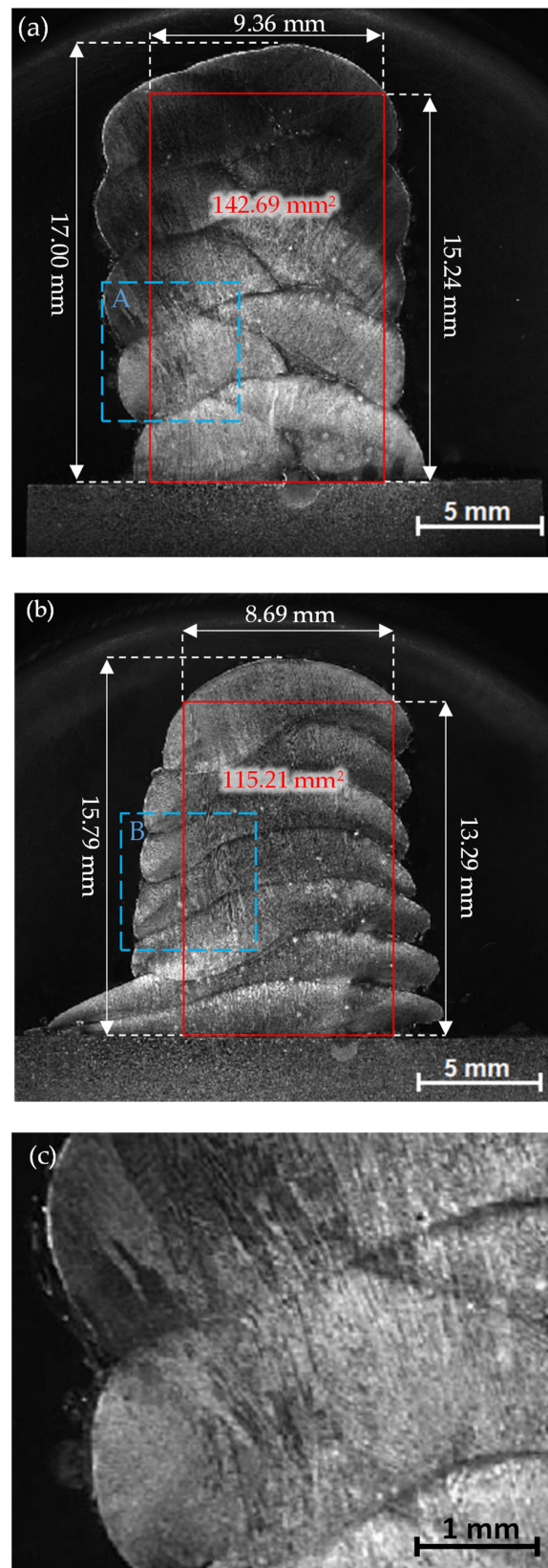


Figure 13. Cont.

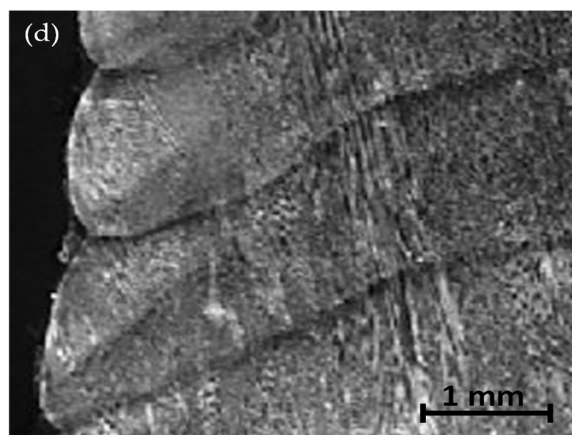


Figure 13. Cross-section of conventional PTA (a), parallel configuration tandem PTA (b), high magnification of the area A (c), and area B (d) [21].

4. Conclusions and Outlook

The results demonstrate that coatings can be produced with the tandem PTA process at highly efficient levels. The tandem PTA process is a high-performance coating process that also provides control of the deposition performance, powder rate, and powder type of both PTA torches. The main conclusions of the article are:

- Increase in deposition rate of coating per time by a factor of 2.4 compared to single torch coating. This is due to double torch deposition, including the heat accumulation between torches for deposition.
- Because of the distance-adjustable double torch setup, the parallel tandem PTA configuration is useful for manufacturing large components with expanded layer width and high deposition rates.
- Due to reduced torch pathway (only 7 instead of 10 seams) and symmetrical manufacture of the wall by double torches, there is a 56% increase in deposition capacity with inline manufacture of tandem PTA.
- The tandem PTA series configuration with multi-material deposition achieves a high surface hardness, which improves wear resistance. Because different materials can be fed into the desired location in the weld pool, it is also possible to achieve a low clad material hardness, which suppresses crack formation.

For example, a ship propeller could be manufactured as an industrial application possibility by tandem PTA. A propeller needs a very hard layer resistant to cavitation damage on the one hand and a soft base body or a crack-resistant surface on the opposite side. On the one hand, the tandem PTA process can be used to produce rapid prototypes of propellers very quickly, and on the other hand, exactly this desired hardness gradient can be realized through multi-material deposition.

Author Contributions: Conceptualization, G.E. and A.H.; methodology, G.E. and A.H.; experimental performing, G.E.; formal analysis, G.E. and A.H.; writing—original draft preparation, G.E.; writing—review and editing, G.E., A.H., J.H., S.H. and J.B.; supervision, S.H., J.H.; All authors have read and agreed to the published version of the manuscript.

Funding: This article was written as part of the “Central Innovation Program” as a cooperative project between the Chemnitz University of Technology and Plasmastar GmbH under the funding code ZF4012624FH8 and the title “Development and evaluation of tandem plasma transferred arc welding process for the efficient coating of free-form surfaces-tandem PTA”.

Institutional Review Board Statement: Not applicable.

Informed Consent Statement: Not applicable.

Data Availability Statement: Not applicable.

Acknowledgments: The authors would like to thank Lars Ohlensehen for preparing the experimental set-up and Avantika Jhanji for help with the language revision.

Conflicts of Interest: The authors declare no conflict of interest.

References

1. Ertugrul, G.; Hälsig, A.; Liu, X.; Kusch, M. Effizientes Beschichten durch Tandem-Plasma-Pulver-Auftragsschweißen. In *DVS Congress 2020 Große Schweißtechnische Tagung, DVS-Berichte*; DVS Media GmbH: Düsseldorf, Germany, 2021; Volume 365, pp. 68–694, ISBN 978-3-96144-098-6.
2. Gebert, A.; Wocilka, D.; Bouaifi, B.; Alaluss, K.; Matthes, K.-J. Neuentwicklungen für den Verschleiß- und Korrosionsschutz beim Plasma-Pulver-Auftragsschweißen. *Mater. Werkst.* **2008**, *39*, 99–104. [\[CrossRef\]](#)
3. Deuis, R.L.; Yellup, J.M.; Subramanian, C. Metal-Matrix Composite Coatings by PTA Surfacing. *Compos. Sci. Technol.* **1998**, *58*, 299–309. [\[CrossRef\]](#)
4. Hoefer, K.; Nitsche, A.; Abstoss, K.G.; Ertugrul, G.; Haelsig, A.; Mayr, P. Correction to: Multi-material Additive Manufacturing by 3D Plasma Metal Deposition for Graded Structures of Super Duplex Alloy 1.4410 and the Austenitic Corrosion Resistant Alloy. *JOM* **2019**, *71*, 2136. [\[CrossRef\]](#)
5. Aldalur, E.; Veiga, F.; Suárez, A.; Bilbao, J.; Lamikiz, A. High deposition wire arc additive manufacturing of mild steel: Strategies and heat input effect on microstructure and mechanical properties. *J. Manuf. Process.* **2020**, *58*, 615–626. [\[CrossRef\]](#)
6. Witzel, J.M.F. Qualifizierung des Laserstrahl-Auftragsschweißens zur Generativen Fertigung von Luftfahrtkomponenten. Master's Thesis, RWTH Aachen University, Aachen, Germany, 2014.
7. Bai, J.Y.; Yang, C.L.; Lin, S.B.; Dong, B.L.; Fan, C.L. Mechanical properties of 2219-Al components produced by additive manufacturing with TIG. *Int. J. Adv. Manuf. Technol.* **2015**, *86*, 479–485. [\[CrossRef\]](#)
8. Attaran, M. The rise of 3-D printing: The advantages of additive manufacturing over traditional manufacturing. *Bus. Horiz.* **2017**, *60*, 677–688. [\[CrossRef\]](#)
9. Rosli, N.A.; Alkahari, M.R.; bin Abdollah, M.F.; Maidin, S.; Ramli, F.R.; Herawan, S.G. Review on effect of heat input for wire arc additive manufacturing process. *J. Mater. Res. Technol.* **2021**, *11*, 2127–2145. [\[CrossRef\]](#)
10. Müller, J.; Grabowski, M.; Müller, C.; Hensel, J.; Unglaub, J.; Thiele, K.; Kloft, H.; Dilger, K. Design and Parameter Identification of Wire and Arc Additively Manufactured (WAAM) Steel Bars for Use in Construction. *Metals* **2019**, *9*, 725. [\[CrossRef\]](#)
11. Zergiebel Schweißtechnik. Plasma-Pulver-Auftragsschweißen (PPA). Available online: <https://www.zergiebel.de/leistungsuebersicht/schweissverfahren/plasma-pulver-auftragsschweissen-ppa.html> (accessed on 13 October 2020).
12. Ertugrul, G.; Hälsig, A.; Kusch, M.; Ohlensehnen, L. Tandem PPA—Leistungssteigerung und beanspruchungsgerechte Beschichtungen. In *DVS Congress 2021 Große Schweißtechnische Tagung, DVS Berichte*; DVS Media GmbH: Düsseldorf, Germany, 2021; Volume 371, pp. 56–63, ISBN 978-3-96144-146-4.
13. Ertugrul, G.; Hälsig, A.; Kusch, M.; Ohlensehnen, L. *Entwicklung und Evaluierung des Tandem Plasma Pulver Auftragsschweißens für Beschichtungen und additive Fertigung* In 41. Assistentenseminar Fügetechnik, DVS Berichte; DVS Media GmbH: Düsseldorf, Germany, 2021; Volume 370, pp. 45–50, ISBN 978-3-96144-141-9.
14. Kaboli, R.; Farid, M.M.; Kramer, R.; Ertugrul, G.; Mayr, P. Numerical Investigation on the Influence of Welding Parameters on the Weld Pool Dynamics and the Distribution of Second Phase Particles. In *Proceedings of the Mathematical Modelling of Weld Phenomena*, Graz, Austria, 23–26 September 2018.
15. Ramkumar, K.D.; Singh, A.; Raghuvanshi, S.; Bajpai, A.; Solanki, T.; Arivarasu, M.; Arivazhagan, N.; Narayanan, S. Metallurgical and mechanical characterization of dissimilar welds of austenitic stainless steel and super-duplex stainless steel—A comparative study. *J. Manuf. Process.* **2015**, *19*, 212–232. [\[CrossRef\]](#)
16. Erdogan, F. Fracture Mechanics of Functionally Graded Materials. *J. Comp. Eng.* **1995**, *5*, 753–770. [\[CrossRef\]](#)
17. Knoll, H.; Ocylok, S.; Weisheit, A.; Springer, H.; Jägle, E.; Raabe, D. Combinatorial Alloy Design by Laser Additive Manufacturing. *Steel Res. Int.* **2016**, *88*, 1600416. [\[CrossRef\]](#)
18. Sampath, S.; Herman, H.; Shimoda, N.; Saito, T. Thermal Spray Processing of FGMs. *MRS Bull.* **1995**, *20*, 27–31. [\[CrossRef\]](#)
19. Zhang, S.; Wang, S.; Wu, C.; Zhang, C.; Guan, M.; Tan, J. Cavitation erosion and erosion-corrosion resistance of austenitic stainless steel by plasma transferred arc welding. *Eng. Fail. Anal.* **2017**, *76*, 115–124. [\[CrossRef\]](#)
20. Hilmas, G.E.; Lombardi, J.L.; Hoffman, R.A. Advances in the Fabrication of Functionally Graded Materials Using Extrusion Freeform Fabrication. In *Functionally Graded Materials 1996, Proceedings of the 4th International Symposium on Functionally Graded Materials, Tsukuba, Japan, 21–24 October 1996*; Ichiro, S., Yoshinari, M., Eds.; Elsevier B.V.: Amsterdam, The Netherlands, 1997; pp. 319–324.
21. Ertugrul, G.; Hälsig, A.; Kusch, M. High deposition additive manufacturing by tandem plasma transferred arc welding. *J. Addit. Manuf. Technol.* **2021**, *1*, 1–4. [\[CrossRef\]](#)
22. Deutsche Edelstahlwerke Services GmbH, Acidur 4301 Technical Data Sheet 1.4301 According to DIN EN 10088-3. 2015. Available online: https://www.dew-stahl.com/fileadmin/files/dew-stahl.com/documents/Publikationen/Werkstoffdatenblaetter/RSH/1.4301_de.pdf (accessed on 24 June 2022).
23. Deutsche Edelstahlwerke Services GmbH, Technical Data Sheet According to EN 10204-2.2. 2019, batch number: 257704. Available online: <https://www.dew-stahl.com/produkte> (accessed on 24 June 2022).

24. Deutsche Edelstahlwerke Services GmbH, Acidur 4404 Technical Data Sheet 1.4404 According to DIN EN 10088-3. 2016. Available online: https://www.dew-stahl.com/fileadmin/files/dew-stahl.com/documents/Publikationen/Werkstoffdatenblaetter/RSH/1.4404_de.pdf (accessed on 24 June 2022).
25. Kotecki, D.; Siewert, T. WRC-1992 constitution diagram for stainless steel weld metals: A modification of the WRC-1988 diagram. *Weld J.* **1992**, *71*, 171–178.